Absence of Scaling for the Intermediate Scattering Function of a Hard-Sphere Suspension: Static and Dynamic X-Ray Scattering from Concentrated Polystyrene Latex Spheres

L. B. Lurio, D. Lumma, A. R. Sandy, M. A. Borthwick, P. Falus, and S. G. J. Mochrie
Center for Materials Science and Engineering, Massachusetts Institute of Technology, Cambridge, Massachusetts 02139-4307

J. F. Pelletier and M. Sutton
Department of Physics, McGill University, Montréal, Québec, H3A 2T8, Canada

Lynne Regan
Department of Molecular Biophysics and Biochemistry, Yale University, New Haven, Connecticut 06520

A. Malik and G. B. Stephenson
Materials Science Division, Argonne National Laboratory, Argonne, Illinois 60439-4832
Received 14 June 1999

X-ray photon correlation spectroscopy and small-angle scattering measurements are presented of the dynamics and structure of concentrated suspensions of charge-stabilized polystyrene latex spheres dispersed in glycerol, for volume fractions from 3% to 52%. The static structures of the suspensions show essentially hard-sphere behavior, and the short-time dynamics shows good agreement with predictions for the wave-vector-dependent collective diffusion coefficient. However, the intermediate scattering function is found to violate a scaling behavior found previously for a sterically stabilized hard-sphere suspension [P. N. Segrè and P. N. Pusey, Phys. Rev. Lett. **77**, 771 (1996)].

The ability to prepare suspensions of nearly perfectly spherical, highly monodisperse nanoscale particles in a liquid enables experiments on accurate realizations of hard spheres. Prototypical systems include polymer and silica colloids with steric or charge stabilization. The static behavior of these colloids closely resembles that of simple liquids. However, their dynamics show significant differences: particle motion is diffusive rather than ballistic, and the particles experience hydrodynamic coupling to near neighbors via disturbances in the suspending medium. Hydrodynamic interactions play an important role for diffusion, although they do not affect the static structure. Indeed, the difficulty of fully treating near-field many-body hydrodynamic interactions remains a principal obstacle to the detailed theoretical understanding of these systems.

Recently, Segrè and Pusey [1] studied dispersions of poly(methylmethacrylate) (PMMA) spheres, sterically stabilized with a grafted layer of poly(hydroxysteric acid) (PHSA), suspended in decalin/tetralin, which have been shown to be excellent hard spheres [2]. They found that the long-time wave-vector-dependent diffusion coefficient (D_L) was accurately proportional to the short-time diffusion coefficient (D_S) over the entire range of wave vectors studied from $QR \simeq 1$ to $QR \simeq 6$, where Q is the scattering vector and R is the sphere radius. Beyond this, they showed that the intermediate scattering function itself displayed a certain scaling behavior for wave vectors greater than $QR \simeq 2.5$. In this paper, however, we show that the scaling observed by Segrè and Pusey is absent for concentrated dispersions of charge-stabilized polystyrene (PS) spheres in glycerol, which, insofar as their static structure is concerned, exhibit behavior indistinguishable from that of hard spheres. We suggest that this discrepancy may result from differences in the fluid flow at the surfaces of charge and sterically stabilized hard spheres.

Because of the refractive index difference between polystyrene ($n \simeq 1.59$) and glycerol ($n \simeq 1.47$), our suspensions are milky in appearance, as a result of strong multiple scattering of light. Consequently, studies of the static correlations and the dynamic mode structure would be very difficult using static and dynamic light scattering. Instead, we have applied the emerging technique of x-ray photon correlation spectroscopy, which applies the principles of dynamic light scattering in the x-ray regime [3–7]. We believe the present results represent an important step in the maturation of this new technique. To characterize the static structure, we performed simultaneous small-angle x-ray scattering (SAXS) measurements.

PS spheres in glycerol constitute a prototypical colloidal system, for which Derjaguin-Landau-Verwey-Overbeek (DLVO) interactions, consisting of a screened electrostatic repulsion between charges at the spheres' surfaces plus a longer-ranged, attractive van der Waals component [8,9], are representative of a large class of colloids. Colloidal particles interacting via DLVO interactions are frequently taken to have effectively hard-sphere interactions [10,11]. This hypothesis has found recent support in elegant experiments, demonstrating that screened, charged polystyrene colloids behave according to the hard-sphere equation of state [12]. Our SAXS measurements, described below, demonstrate that the interactions between PS spheres in glycerol are indistinguishable from those of hard spheres.

An aqueous suspension containing PS latex particles with a nominal radius of 71 nm was purchased from Duke Scientific. The relative standard deviation in radius was 0.025. Known weights of the as-received suspension were mixed with known weights of glycerol. Water was then removed by evaporation under vacuum. Glycerol was chosen to slow the dynamics, permitting time-resolved scattering measurements using a CCD detector [3,6]. Samples were manufactured with nominal sphere volume fractions of $\phi = 0.027$, 0.13, 0.28, 0.34, 0.49, and 0.52. For the x-ray experiments, samples were mounted in an evacuated, temperature-controlled sample chamber and cooled to $-5\,^{\circ}\mathrm{C}$.

The measurements were carried out at beam line 8-ID at the Advanced Photon Source (APS). Details of the setup are presented elsewhere [13]. Briefly, we employed x rays of energy 7.66 keV produced by a 72-pole undulator. A silicon mirror and germanium monochromator selected a relative energy bandwidth of 3×10^{-4} full width at half maximum. Subsequently, a pair of precision crossed slits, 55 m from the undulator source and 40 cm upstream of the sample, selected a 20 μm horizontal by 50 μm vertical portion of the beam. The resulting partially coherent flux on the sample was $\sim 10^{10}$ photons per second. Scattered x rays were detected 4.85 m farther downstream using the CCD detector.

The time- and circularly-averaged x-ray scattering cross sections are displayed in Fig. 1 for wave vectors from $QR = 1$ to $QR = 10$ for each sample. At large wave vectors the shape of the scattering appears independent of volume fraction and shows intensity oscillations characteristic of uniform spheres. The solid line in Fig. 1 shows the best fit to the $\phi = 0.027$ data of a model for the scattering of hard spheres with a volume fraction of 0.027 and a relative polydispersity in radius of 0.025 [14], convoluted with our experimental resolution. The sole fitting parameter was the mean particle radius, resulting in a best-fit value of 66.5 nm, in fair agreement with the manufacturer's value. The model provides a good description of the data for $QR < 3$. However, significant deviations from the theoretical form appear at the scattering minima. We ascribe the discrepancy to small departures of the latex particles from spherical symmetry. Similar behavior was observed in Ref. [15].

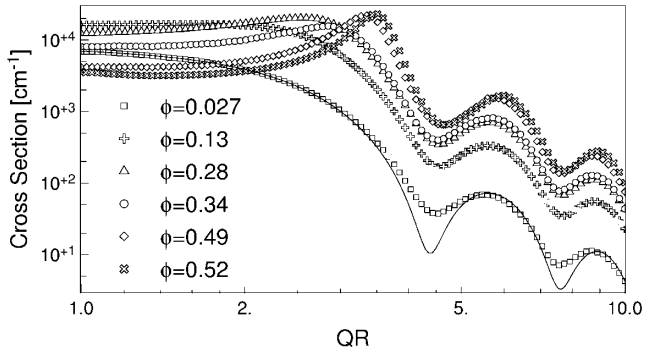

FIG. 1. Cross section for several different volume fractions of PS spheres in glycerol vs QR.

A pronounced peak develops near $QR \simeq 3.5$ as the volume fraction increases, corresponding to increasing interparticle correlations. This behavior is highlighted in Fig. 2, which shows as the open circles the structure factors, $S(Q)$, for each sample, obtained by dividing the measured scattering by the particle form factor, for which we used the measured scattering from the $\phi = 0.027$ sample after applying a small correction for the structure factor. The principal peak of the structure factor approaches $QR \simeq 3.5$ at large volume fractions, consistent with what may be expected for hard spheres. By contrast, particles with long-ranged Coulomb repulsions would exhibit a larger mean separation, a first peak of the structure factor at smaller wave vectors, and greater ordering at low volume fractions.

The dashed lines in Fig. 2 correspond to the model hard-sphere structure factor for particles with a mean radius of $R = 66.5$ nm and a polydispersity in radius of 0.025 [14], fitted to the measured structure factor, varying only the volume fraction for each data set. Evidently, the model provides a good description of the experimental structure factors at all volume fractions, in particular reproducing the position of the principal peak accurately. The best-fit values for the volume fractions of the different samples are indistinguishable from the nominal volume fractions. It is especially notable that the behavior of the

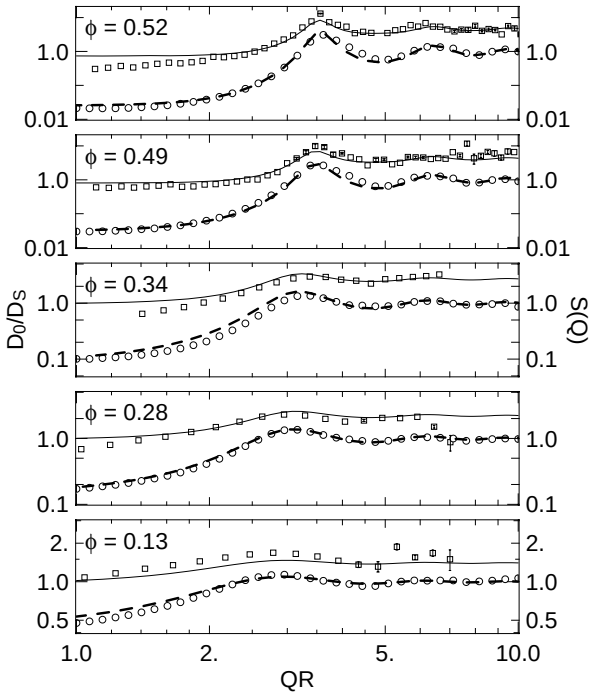

FIG. 2. Measured and model structure factors $S(Q)$ (circles and dashed lines, respectively), and short-time diffusion coefficients relative to the Einstein-Stokes diffusion coefficient D_S/D_0 (squares and solid lines, respectively) vs QR for PS spheres in glycerol.

measured structure factor at small wave vectors is reproduced well—within 10%—by the model. This informs us that the osmotic compressibility of PS spheres in glycerol is well described by the hard-sphere equation of state [8]. We view the agreement between the model and measured structure factors at small wave vectors, as well as the agreement between the measured and predicted positions of the principal peak in the structure factor, as convincing evidence that PS spheres in glycerol manifest hard-sphere configurations.

Dynamical properties of the suspensions were characterized via autocorrelation of sequences of CCD images, and normalized to the circular average of the CCD scattering at each wave vector. In this way, we are able to determine the normalized intensity-intensity autocorrelation function, $g_2(Q,t)$, which is related to the normalized intermediate scattering function, $f(Q,t)$, via [8]

$$g_2(Q,t) = 1 + A[f(Q,t)]^2, \tag{1}$$

where t is the delay time, and A is a setup-dependent contrast [16]. For the present measurements, A is about 0.1.

Representative intensity autocorrelations are shown over delay times from 30 ms to 300 s for samples with $\phi = 0.28$ and $\phi = 0.52$ obtained at $QR = 1.5$, 3.5, and 6.0 in Figs. 3(a) and 3(b), respectively. In a dilute suspension, the diffusion equation describes the low-frequency dynamics, predicting that density fluctuations relax exponentially in time, with a relaxation rate given by $f(Q,t) = \exp(-D_0Q^2t)$, where $D_0 = k_BT/6\pi\eta R$, with η the viscosity of the suspending medium. For moderate volume fractions, the relaxation remains exponential, but the diffusion coefficient deviates from the isolated particle value. For $\phi = 0.28$, single-exponential fits to the form $f = \exp(-D_SQ^2t)$, shown as the solid lines in Fig. 3(a), provide an excellent description of the measured intensity autocorrelations versus delay time. Similarly, for the samples with volume fractions of $\phi = 0.027$ and 0.13 (data not shown), a single-exponential decay works well. At higher-volume fractions the intermediate scattering functions exhibit more complex time dependence. In this case it is possible to define a time-dependent diffusion coefficient via

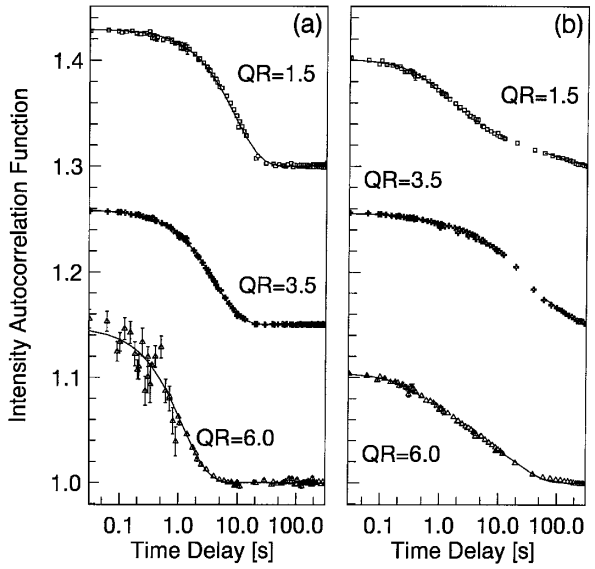

FIG. 3. Intensity time autocorrelation functions, $g_2(Q,t)$, for PS spheres in glycerol with volume fractions of (a) $\phi = 0.28$ and (b) $\phi = 0.52$ for $QR = 1.5$ (offset by 0.3), 3.5 (offset by 0.15), and 6.0. Lines correspond to the models described in the text.

$$D(Q,t) = \frac{-1}{Q^2}\frac{\partial \ln[f(Q,t)]}{\partial t}. \tag{2}$$

We find that at both short and long times $\ln(f)$ varies linearly with t, so that, following Segrè and Pusey, we may introduce corresponding short-time and long-time diffusion coefficients: $D_S = D(Q,0)$ and $D_L = D(Q,\infty)$, respectively. We determined the short- and long-time diffusion coefficients by linear least squares fits over time ranges at short and long times, respectively, in which $\ln(f)$ does not deviate significantly from a straight line. In Fig. 3(b), the solid lines illustrate the corresponding model intensity autocorrelations plotted over the time ranges in question. Clearly, in these time ranges, the model autocorrelations describe the data well.

Displayed in Fig. 2 as the open squares is D_0/D_S versus wave vector for each sample obtained from the slope of $\ln[f(Q,t)]$ at small times. The most striking feature of these and earlier [17–22] results is that the inverse of the diffusion coefficient displays a peak that mimics the peak in the static structure factor, informing us that configurations of low free energy are also long lived. This link between structure and dynamics is well known as "de Gennes narrowing." In the absence of hydrodynamic interactions the wave-vector dependence of the inverse diffusion coefficient would result entirely from the static structure factor [23]. Since it is clear from Fig. 2 that D_0/D_S and $S(Q)$ are not identical, significant hydrodynamic interactions are indicated. Moreover, since $D_0/D_S > S(Q)$, we may infer that hydrodynamic interactions inhibit diffusion at all wave vectors. Analytic calculations of the wave-vector dependence of D_0/D_S for hard spheres, taking into account many-body hydrodynamic interactions, have been carried out by Beenakker and Mazur [24]. Extrapolations of their predictions onto the present measurements are illustrated as the solid lines in Fig. 2. Our data exhibit good agreement at intermediate volume fractions. At high volume fractions, there is an additional slowing down in the vicinity of the peak in the structure factor. This effect, also seen by Segrè, Behrend, and Pusey [21], is consistent with their computer simulations for hard spheres based on the fluctuating lattice Boltzmann equation. We take this agreement of the short-time diffusion coefficients as further evidence that the interactions between PS particles in glycerol are hard sphere in character.

The scaling behavior found by Segrè and Pusey is that, at fixed volume fraction, the intermediate scattering function is independent of wave vector after scaling by the initial decay rate $D_S(Q)Q^2$ between $QR = 2.5$ and $QR = 6.0$. Figure 4(a) shows our results for the intermediate scattering function scaled using the diffusion coefficients from Fig. 2 for $\phi = 0.13$ and 0.49. The low volume fraction data scales to a straight line with a slope of -1. By contrast, at $\phi = 0.49$, the data deviate from a straight line. More significantly, these data do not collapse to a single scaling form. Also shown as dashed lines are the linear fits to the long-time tails of $\ln(f)$. The violation of scaling is quantified in Fig. 4(b) which details the wave-vector dependence of the ratio of the short- and long-time diffusion coefficients $D_S(Q)/D_L(Q)$, for high volume fractions. The proposed scaling requires that this ratio remain independent of wave vector. By contrast, in the present measurement this ratio shows a strong wave-vector dependence in the vicinity of the structure factor peak, and a weaker variation with wave vector at both smaller and larger values.

In conclusion, we have presented a detailed dynamic and static x-ray scattering study of diffusion and structure in a concentrated suspension of hard spheres: PS latex spheres in glycerol. We do not find scaling behavior of the intermediate scattering function. The discrepancies between the results of Ref. [1] and our measurements may be an indication that the dynamical behavior of sterically stabilized systems is distinct from that of charge-stabilized systems, even though differences in the static structure are negligible. Perhaps the projecting polymer strands used to produce the steric stabilization in the PMMA system lead to a stickier flow boundary. In this regard, it may be pertinent to recall the observation [2] that the low-shear-rate viscosities of "hard-sphere dispersions" appear to fall into two bands. The higher viscosity band includes the results of several measurements performed on PMMA-PHSA dispersions; the lower viscosity band includes measurements on PS and silica suspensions in both aqueous and nonaqueous liquids.

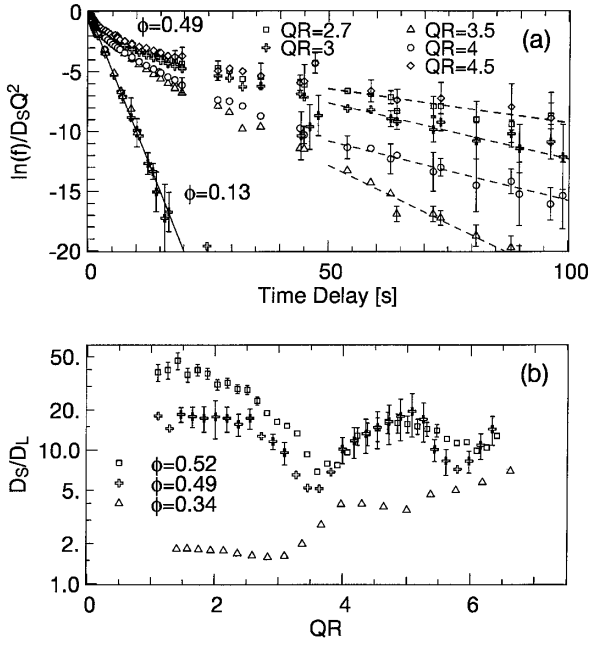

FIG. 4. (a) Scaled intermediate scattering functions at several wave vectors for samples with $\phi = 0.49$ and 0.13. Symbols are experimental data. The solid line corresponds to a slope of -1. The dashed lines correspond to the fits described in the text. (b) Ratio of short-time and long-time diffusion coefficients.

8-ID was developed with support from the NSF Instrumentation for Materials Research Program (DMR 9312543), from the DOE Facilities Initiative Program (DE-FG02-96ER45593), and from NSERC. Work at MIT was also supported by the NSF MRSEC Program (DMR 9808941). D. L. acknowledges the JSEP for support. The APS is supported by the DOE under Contract No. W-31-109-Eng-38. We thank Bruce Ackerson, Harold Gibson, and Aleksey Lomakin for their invaluable assistance, and Benjamin Chu for helpful comments.

[1] P. N. Segrè and P. N. Pusey, Phys. Rev. Lett. **77**, 771 (1996).
[2] S.-E. Phan *et al.,* Phys. Rev. E **54**, 6633 (1996).
[3] S. Dierker *et al.,* Phys. Rev. Lett. **75**, 449 (1995).
[4] T. Thurn-Albrecht *et al.,* Phys. Rev. Lett. **77**, 5437 (1996).
[5] S. G. J. Mochrie *et al.,* Phys. Rev. Lett. **78**, 1275 (1997).
[6] O. K. C. Tsui and S. G. J. Mochrie, Phys. Rev. E **57**, 2030 (1998).
[7] A. C. Price *et al.,* Phys. Rev. Lett. **82**, 755 (1999).
[8] P. N. Pusey, *Liquids, Freezing and the Glass Transition* (North-Holland, Amsterdam, 1991).
[9] W. C. K. Poon and P. N. Pusey, in *Observation, Prediction, and Simulation of Phase Transitions in Complex Fluids,* edited by M. Baus (Kluwer, Dordrecht, 1995).
[10] M. H. Kao, A. G. Yodh, and D. J. Pine, Phys. Rev. Lett. **70**, 242 (1993).
[11] T. G. Mason and D. A. Weitz, Phys. Rev. Lett. **75**, 2770 (1995).
[12] M. A. Rutgers *et al.,* Phys. Rev. B **53**, 5043 (1996).
[13] D. Lumma *et al. (*unpublished).
[14] W. L. Griffith, R. Triolo, and A. L. Compere, Phys. Rev. A **35**, 2200 (1987).
[15] B. Chu, Y. Li, P. J. Harney, and F. Yeh, Rev. Sci. Instrum. **64**, 1510 (1994).
[16] A. R. Sandy *et al.,* J. Synchrotron Radiat. **6**, 1174 (1999).
[17] J. C. Brown, P. N. Pusey, J. W. Goodwin, and R. H. Ottewill, J. Phys. A **8**, 664 (1975).
[18] F. Grüner and W. Lehmann, J. Phys. A **12**, L303 (1979).
[19] W. van Megan, R. H. Ottewill, S. M. Owens, and P. N. Pusey, J. Chem. Phys. **82**, 508 (1985).
[20] A. P. Philipse and A. Vrij, J. Chem. Phys. **88**, 6459 (1988).
[21] P. N. Segre, O. P. Behrend, and P. N. Pusey, Phys. Rev. E **52**, 5070 (1995).
[22] J. K. Phalakornkul *et al.,* Phys. Rev. E **54**, 661 (1996).
[23] W. Hess and R. Klein, Adv. Phys. **32**, 173 (1983).
[24] C. W. J. Beenakker and P. Mazur, Physica (Amsterdam) **126A**, 349 (1984).